IX CONGRESSO BRASILEIRO DE ENGENHARIA E CIÊNCIAS TÉRMICAS

9th BRAZILIAN CONGRESS OF THERMAL ENGINEERING AND SCIENCES

Paper CIT02-0803

ANALYSIS OF TOLLMIEN-SCHLICHTING WAVES PROPAGATION ON A FLAT PLATE WITH A NAVIER-STOKES SOLVER

Leandro F. de Souza
Instituto Tecnológico de Aeronáutica
Pç Mal. Eduardo Gomes, 50 - São José dos Campos, SP - 12228 900, Brazil
lefraso@zipmail.com.br

Márcio T. Mendonça
Centro Técnico Aeroespacial, Instituto de Aeronáutica e Espaço
Pç Mal. Eduardo Gomes, 50 - São José dos Campos, SP - 12228 904, Brazil
marcio_tm@yahoo.com

Marcello A. Faraco de Medeiros
USP - Universidade de São Paulo
Escola de Engenharia de São Carlos - Departamento de Engenharia Aeronáutica
Av. Trabalhador São Carlense, 400 - SP - 13566-590, Brazil
marcello@sc.usp.br

Markus Kloker
Institut für Aerodynamik und Gasdynamik - Universität Stuttgart
Stuttgart, Germany
mkloker@iag.uni-stuttgart.de

Abstract. *A numerical method for accurately solving the incompressible Navier-Stokes equation in vorticity-velocity formulation is presented. The governing equations are discretized using a sixth order compact finite differences scheme for the spatial derivatives. The Poisson equation for the normal velocity component is solved by an iterative Line Successive Over Relaxation Method using a multigrid Full Approximation Scheme to accelerate the convergence. Results are presented for the spatial evolution of two-dimensional Tollmien-Schlichting waves on a flat plate boundary layer with a very small disturbance amplitude. Growth rates, phase and eigenfunctions are compared with results from Linear Stability Theory, providing a through check of the numerical method. Finite amplitude disturbances are also considered. The main interest in a two-dimensional nonlinear instability analysis is to use it as a step toward a three dimensional code. Nonlinear results are compared against results obtained from a code based on the Parabolized Stability Equations.*

Key words: *Boundary layer stability, Compact differences schemes, Vorticity-velocity formulation, Hydrodynamic instability, Laminar flow transition.*

1. Introduction

Laminar-turbulent transition is one of the areas in fluid mechanics which has a large number of unanswered questions. Nevertheless, there are many scientific and industrial applications in which laminar flow stability and transition to turbulence are relevant. Transition to turbulence may increase skin friction and wall heat transfer, but also helps avoid boundary layer separation and increase fluid mixing between fuel and oxidizer in combustion devices. Therefore, it is important to investigate the physics of stability and transition in order to control, hasten or prevent it. A large effort has been made in recent years to advance the knowledge in this area.

Among the most recent tools used to study laminar flow stability and transition problems, there are now highly accurate numerical techniques based on the direct numerical simulation of Navier-Stokes equations (DNS) that are able to capture all the relevant temporal and spatial scales. Different approaches have been presented in the literature (Laurien and Kleiser, 1989; Biringen and Laurien, 1991; Spalart, 1989; Gmelin et al., 1999; Meyer et al., 1999; Zhong, 1999; Whang and Zhong, 1999; Hu and Zhong, 1999; Guschin et al., 1999) and the common factor among them is the need of high resolution discretization methods (Zang et al., 1989). The approach based on the vorticity-velocity formulation and on the use of compact differencing schemes is adopted in the current work (Bestek, 1980; Messing et al., 1999; Stemmer and Kloker, 1999; Wassermann and Kloker, 1999; Wassermann and Kloker, 1998; Zhang and Fasel, 1999; Fezer and Kloker, 1999). According to Davies et al., 1999, this choice of dependent variables has some advantages over other formulations and can be easily implemented in a high order finite difference discretization necessary for the solution of instability and transition problems (Farouk and Fusegi, 1985).

This work is part of an ongoing effort to develop a DNS solver that is able to simulate laminar flow instability problems and transition to turbulent flow. The present stage in this development correspond to the implementation of a two-dimensional Navier-Stokes solver capable of accurately represent the propagation of nonlinear Tollmien-Schlichting (TS) waves in boundary layers.

The code is an extension of a previous implementation used to study linear stability of TS waves in a plane Poiseuille flow (Souza et al., 2001). It is based on the vorticity-velocity formulation and on high order compact differencing schemes (Souza et al., 2001, Kopal, 1961, Lele, 1992). The governing equation are discretized in time with a fourth order Runge-Kutta scheme. In space a sixth order compact schemes is used (Lele, 1992; Mahesh, 1998).

The same methodology used in Souza et al., 2001 is now used to compute the propagation of TS waves in boundary layers considering both nonlinear and nonparallel effects (boundary layer growth). In order to handle the more demanding nonlinear problem, and in preparation for the extension to the three-dimensional formulation, a multi-grid scheme has been implemented to speed up convergence of the Poisson solver. Also, an outflow buffer domain technique has been used to avoid wave reflections on the exit boundary.

Results are compared with linear stability theory (LST) (Mendonça, 2000) and with numerical results from a Parabolized Stability Equation (PSE) solver (Mendonça, 2000). The use of nonlinear two-dimensional TS waves is only meaningful as a stepping stone toward a fully three-dimensional simulation. The final objective of this effort is to study boundary layer transition and control for flows over curved surfaces and to develop transition models that can be used in industrial and aerospace applications. In the following sections first the details of the formulation and of the numerical method are presented (Sections 2 and 3). Section 4 presents comparisons with linear stability theory and with nonlinear and nonparallel numerical results obtained with a PSE code for the evolution of Tollmien-Schlichting waves over a flat plate. The conclusions are presented in Section 5.

2. Formulation

The Navier-Stokes equations are written in vorticity-velocity formulation in order to eliminate the pressure terms from the governing equations (Fezer and Kloker, 1999).

The following nondimensional variables are adopted:

$$x = \frac{\bar{x}}{\bar{L}}, \quad y = \frac{\bar{y}}{\bar{L}}\sqrt{Re}, \quad u = \frac{\bar{u}}{\bar{U}_\infty}, \quad v = \frac{\bar{v}}{\bar{U}_\infty}\sqrt{Re}, \quad t = \bar{t}\frac{\bar{U}_\infty}{\bar{L}}, \quad \text{and} \quad Re = \frac{\bar{U}_\infty \bar{L}}{\bar{\nu}}. \tag{1}$$

Where parameters with over-bar are dimensional parameters. $\bar{L}$ is the reference length, $\bar{U}_\infty$ is the maximum velocity, $\bar{\nu}$ is kinematic viscosity and Re is the Reynolds Number.

The vorticity in the spanwise direction, denoted by w_z, is given by:

$$w_z = \frac{\partial u}{\partial y} - \frac{1}{Re}\frac{\partial v}{\partial x}. \tag{2}$$

The vorticity transport equation is given by:

$$\frac{\partial w_z}{\partial t} = -\frac{\partial u w_z}{\partial x} - \frac{\partial v w_z}{\partial y} + \frac{1}{Re}\left(\frac{\partial^2 w_z}{\partial x^2}\right) + \frac{\partial^2 w_z}{\partial y^2}. \tag{3}$$

The continuity equation is given by:

$$\frac{\partial u}{\partial x} + \frac{\partial v}{\partial y} = 0. \tag{4}$$

From the vorticity equation (2) and the continuity equation (4) two Poisson-type equations for the velocities can be derived:

$$\frac{1}{Re}\frac{\partial^2 u}{\partial x^2} + \frac{\partial^2 u}{\partial y^2} = \frac{\partial w_z}{\partial y}. \tag{5}$$

$$\frac{1}{Re}\frac{\partial^2 v}{\partial x^2} + \frac{\partial^2 v}{\partial y^2} = -\frac{\partial w_z}{\partial x}. \tag{6}$$

The governing equations are integrated in a rectangular domain as shown in Fig. (3). In the streamwise direction $x_0 \leq x \leq x_{max}$, and in the wall normal direction $0 \leq y \leq y_{max}$. The fluid enter the domain at $x = x_0$ and exit at $x = x_{max}$.

The following boundary conditions are used for the above governing equations:
at the inflow boundary, the velocity and vorticity components are given by the laminar Blasius solution. At the wall ($y = 0$), the no slip condition is applied and all velocity components are set to zero.

The vorticity at the wall is calculated using the Poisson equation (6). At the wall the second derivative of v in the x direction is zero and the Eq. (6) results:

$$\frac{\partial w_z}{\partial x} = -\frac{\partial^2 v}{\partial y^2}. \tag{7}$$

At the upper boundary the flow is assumed to be irrotational (i.e. vorticity equal zero). The velocities are calculated imposing an exponential decay away from the wall such that:

$$\frac{\partial u}{\partial y} = -\alpha u, \tag{8}$$

$$\frac{\partial v}{\partial y} = -\alpha v. \tag{9}$$

This boundary condition is similar to the boundary condition imposed for the solution of the Orr-Sommerfeld equation in LST. According to Fasel (Fasel et al., 1990), the value of α, the wavenumber of the TS wave, does not have a large influence on the results as long as the value of y_{max} is sufficiently large. The extent of the domain in the normal direction, y_{max} has to be chosen in a way that these conditions are true.

At the outflow ($x = x_{max}$), we set the second derivative of the velocity components with respect to x equal to zero. In doing so we obtain the following expressions:

$$\frac{\partial^2 u}{\partial y^2} = \frac{\partial w_z}{\partial y} \qquad \text{and} \qquad \frac{\partial^2 v}{\partial y^2} = -\frac{\partial w_z}{\partial x}. \tag{10}$$

A damping zone near the outflow boundary is used in which all the disturbances are gradually damped down to zero. This technique is well documented by Kloker et al. (Kloker et al., 1993), where the advantages and requirements are discussed. Meitz and Fasel (Meitz and Fasel, 2000) adopted a fifth order polynomium in their work, and the same function is used in present simulations. The basic idea is to multiply the vorticity by a ramp function after each step of the integration method. This technique has proved to be very efficient in avoiding reflections that could come from the outflow boundary conditions when simulating disturbed flows.

Equations (3) to (6) are solved numerically by the scheme described in the next subsection.

3. Numerical Method

The equations presented in Section 2 are discretized using compact finite differences for the spatial derivatives. A 6^{th} order scheme is used for the interior points and a 5^{th} order scheme is used at the boundaries.

The details of the discretization scheme are as follows (Souza et al., 2001):

For points at the boundary, $i = 1$:

$$f'_1 + 4f'_2 = \frac{1}{24dx}(-74f_1 + 16f_2 + 72f_3 - 16f_4 + 2f_5) + O(dx^5). \tag{11}$$

For the first point next to the boundary, $i = 2$:

$$f'_1 + 6f'_2 + 2f'_3 = \frac{1}{120dx}(-406f_1 - 300f_2 + 760f_3 - 80f_4 + 30f_5 - 4f_6) + O(dx^6). \tag{12}$$

For the points near other boundaries, $i = N$ and $i = N - 1$, similar approximations were used.

For the interior points, a 6^{th} order Padé approximation was used:

$$f'_{i-1} + 3f'_i + f'_{i+1} = \frac{1}{12dx}(-f_{i-2} - 28f_{i-1} + 28f_{i+1} + f_{i+2}) + O(dx^6). \tag{13}$$

The final implicit algebraic system of equations is presented below for the first derivatives in the streamwise direction. Similar expressions are obtained for the derivatives in the normal direction.

$$\begin{bmatrix} 1 & 4 & & & & & \\ 1 & 6 & 2 & & & & \\ & \cdot & \cdot & \cdot & & & \\ & & 1 & 3 & 1 & & \\ & & & \cdot & \cdot & \cdot & \\ & & & & 2 & 6 & 1 \\ & & & & & 4 & 1 \end{bmatrix} \begin{bmatrix} f'_1 \\ f'_2 \\ \cdot \\ f'_i \\ \cdot \\ f'_{N-1} \\ f'_N \end{bmatrix} = \begin{bmatrix} \frac{(-74f_1+16f_2+72f_3-16f_4+2f_5)}{24dx} \\ \frac{(-406f_1-300f_2+760f_3-80f_4+30f_5-4f_6)}{120dx} \\ \cdot \\ \frac{(-f_{i-2}-28f_{i-1}+28f_{i+1}+f_{i+2})}{12dx} \\ \cdot \\ \frac{(406f_N+300f_{N-1}-760f_{N-2}+80f_{N-3}-30f_{N-4}+4f_{N-5})}{120dx} \\ \frac{(74f_N-16f_{N-1}-72f_{N-2}+16f_{N-3}-2f_{N-4})}{24dx} \end{bmatrix}.$$

The second derivative, at the boundary, $i = 1$, were discretized using a 5^{th} order asymmetric approximation:

$$13f''_1 + 137f''_2 = \frac{1}{120dx^2}(9775f_1 - 20285f_2 + 11170f_3 - 550f_4 - 145f_5 + 36f_6) + O(dx^5). \tag{14}$$

The first point near the boundary, $i = 2$, used a 6^{th} order asymmetric approximation:

$$\begin{aligned} f''_1 \quad + \quad & 12f''_2 + 3f''_3 = \\ & \frac{1}{360dx^2}(4834f_1 - 8424f_2 + 1890f_3 + 2320f_4 - 810f_5 + 216f_6 - 26f_7) + O(dx^6) \end{aligned} \tag{15}$$

The interior points used a 6^{th} order Padé approximation:

$$2f''_{i-1} + 11f''_i + 2f''_{i+1} = \frac{1}{4dx^2}(3f_{i-2} + 48f_{i-1} - 102f_i + 48f_{i+1} + 3f_{i+2}) + O(dx^6). \tag{16}$$

For the points near other boundaries, $i = N$ and $i = N - 1$, similar approximations to the ones used for points $i = 1$ e $i = 2$ are used.

The resulting linear algebraic system of equations in matrix form reads:

$$\begin{bmatrix} 13 & 137 & & & & & \\ 1 & 12 & 3 & & & & \\ & \cdot & \cdot & \cdot & & & \\ & & 2 & 11 & 2 & & \\ & & & \cdot & \cdot & \cdot & \\ & & & & 3 & 12 & 1 \\ & & & & & 137 & 13 \end{bmatrix} \begin{bmatrix} f''_1 \\ f''_2 \\ \cdot \\ f''_i \\ \cdot \\ f''_{N-1} \\ f''_N \end{bmatrix} =$$

$$\begin{bmatrix} \frac{1}{120dx^2}(9775f_1 - 20285f_2 + 11170f_3 - 550f_4 - 145f_5 + 36f_6) \\ \frac{1}{360dx^2}(4834f_1 - 8424f_2 + 1890f_3 + 2320f_4 - 810f_5 + 216f_6 - 26f_7) \\ \cdot \\ \frac{1}{4dx^2}(3f_{i-2} + 48f_{i-1} - 102f_i + 48f_{i+1} + 3f_{i+2}) \\ \cdot \\ \frac{1}{360dx^2}(4834f_N - 8424f_{N-1} + 1890f_{N-2} + 2320f_{N-3} - 810f_{N-4} + 216f_{N-5} - 26f_{N-6}) \\ \frac{1}{120dx^2}(9775f_N - 20285f_{N-1} + 11170f_{N-2} - 550f_{N-3} - 145f_{N-4} + 36f_{N-5}) \end{bmatrix}. \tag{17}$$

The subscript i represents the grid position in the x direction, and varies from 1 to N.

To solve the Poisson equation, a Line Successive Over-Relaxation method (LSOR) is used. The method used is a mix of a 4^{th} order explicit approximations in x direction and 6^{th} order compact approximations in y direction. Some tests were made using a full 6^{th} order compact approximations method and no relevant differences in the results were found. The full 6^{th} order compact method required a greater computational effort and was abandoned.

In order to accelerate the convergence a Full Approximation Scheme (FAS) multigrid was implemented. A v-cycle working with 4 grids was implemented. The number of cycles used varies according to the desirable convergence criteria. The adopted criteria was that the residual should be last than 1×10^{-9}. The residual of the v-Poisson equation is:

$$def = -\frac{1}{Re}\frac{\partial^2 v}{\partial x^2} - \frac{\partial^2 v}{\partial y^2} - \frac{\partial w_z}{\partial x}. \tag{18}$$

A classical fourth order Runge-Kutta scheme was adopted for the time integration. At each step of the Runge-Kutta the following instructions are necessary:

1. Compute the Right Hand Side (RHS) of the vorticity transport equation (3);
2. Integrate the vorticity transport equation over one sub step;
3. Apply the buffer domain technique near the outflow boundary;
4. Calculate v velocity from the v-Poisson equation (6);
5. Calculate u velocity from the continuity equation (4);
6. Calculate the vorticity generation at the wall using the new velocity distribution.

Steady State Simulation: The unsteady computation starts from a steady state laminar solution. A Blasius solution could have been used to start the computation, but in order to avoid transients in the first steps of the numerical solution the code itself was used to arrive at a steady state solution. The boundary layer approximation would introduce an error of the order of $1/Re$.

To integrate Eq. (3) to a steady state in time, a second order predictor corrector scheme was implemented. Since this scheme is implemented to reach the steady state solution, where the time derivative is zero, any other integration scheme can be used here.

Unsteady Simulation: To simulate the propagation of Tollmien-Schlichting waves in a boundary layer, we must introduce a disturbance in the computational field. In order to do that it is necessary to change the boundary conditions at the wall.

In experimental studies of Tollmien-Schlichting waves the disturbances are introduced in the flow through a vibrating ribbon located shortly downstream of the leading edge (Medeiros and Gaster, 1999). In numerical studies this waves can be introduced at the inflow, using for that the eigenfunctions obtained by an Orr-Sommerfeld equation solver (Souza et al., 2001). The disturbances may be introduced at the wall, through a periodic blowing and suction strip. According to Fasel (Fasel et al., 1990) the second method has proved to be a very efficient method to introduce this kind of disturbance. In this work the second method was adopted. The method consist of introducing a slot at the wall ($i_1 \leq i \leq i_2$), where i_1 and i_2 are the first and the last point of the disturbance strip, respectively. The function used for the normal velocity v is:

$$\begin{aligned} v(i,0,t) = f(x)_i A\sqrt{Re}\sin(\beta t+\theta) \qquad &\text{for} \qquad i_1 \leq i \leq i_2 \\ &\text{and} \\ v(x,0,t) = 0 \qquad \text{for} \qquad i_2 \leq i \quad &\text{and} \quad \leq i_1 \end{aligned} \tag{19}$$

The values of A and θ are real constants that can be chosen to adjust the amplitude and phase of the blowing and suction disturbances. The constant β is the dimensionless frequency. The function $f(x)_i$ adopted here is a fifth order function, and was proposed by Zhang and Fasel (Zhang and Fasel, 1999). The function is:

$$\begin{aligned} f(x)_i &= \frac{1}{48}(729\epsilon^5 - 1701\epsilon^4 + 972\epsilon^3) \qquad \text{if} \qquad i_1 \leq i \leq \frac{1}{2}(i_1+i_2) \\ \text{where} \qquad &\epsilon = 2\frac{i-i_1}{i_2-i_1} \\ f(x)_i &= \frac{-1}{48}(729\epsilon^5 - 1701\epsilon^4 + 972\epsilon^3) \qquad \text{if} \qquad \frac{1}{2}(i_1+i_2) \leq i \leq i_2 \\ \text{where} \qquad &\epsilon = 2\frac{i_2-i}{i_2-i_1} \end{aligned} \tag{20}$$

The shape of the function $f(x)_i$ and its second derivative at the blowing and suction region are plotted in Figs. (1) and (2).

Now we have a disturbance strip at the wall where the normal velocity component is different from zero. The v velocity distribution at the wall is fixed at each time step according to Eq. (20). The vorticity calculation at this boundary also changes, because the second derivative of the v velocity in streamwise direction has a value in the disturbance strip region. This value can be evaluated analytically from Eq. (20).

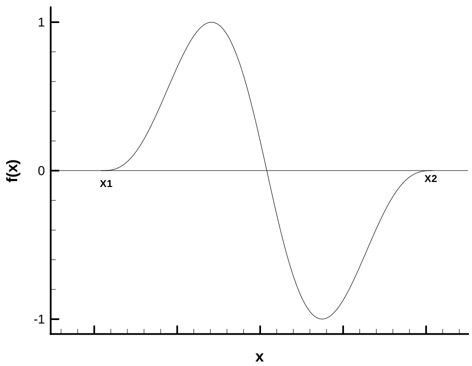

Figure 1: Normal velocity distribution at the suction and blowing region.

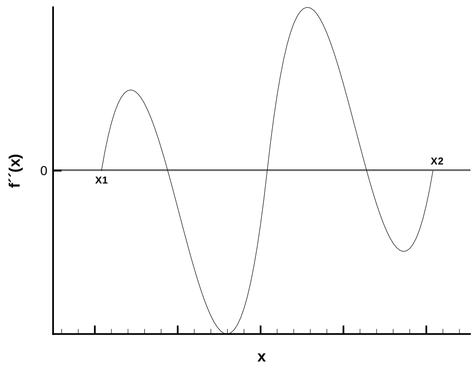

Figure 2: Second derivative of the normal velocity distribution at the suction and blowing region.

4. Numerical Results

In order to check if the code is able to simulate the propagation of disturbances in a flat plate boundary layer, a very small amplitude disturbance was introduced. This allowed the comparison with Linear Stability Theory, providing a through check of the numerical method. Then, a finite disturbance was introduced and after performing a Fourier analysis, the results were compared to results obtained with a code based on parabolized stability equations (Mendonça, 2000). In the computations discussed here, the following parameters were used:

$$U_{\text{inf}} = 30 \ \text{m/s}, \ L = 5 \times 10^{-2} \ \text{m}, \ \nu = 1.5 \times 10^{-5} \ \text{m}^2/\text{s}, \ \text{and} \ Re = 10^5. \tag{21}$$

The frequency F is defined as $F = (\beta/Re) \times 10^4$.

The integration domain used for all tests is shown in Fig. (3). It extends from $x_0 = 0.683$ to $x_{max} = 6.443$ in the streamwise direction and from $y_0 = 0$ to $y_{max} = 32.39$ in the normal direction. The number of points used was 513 and 113 in x and y direction respectively. In time 50 steps were used per wave period. The disturbances were generated between $x_1 = 0.908$ and $x_2 = 1.133$. The frequency used was $F = 10$. After 24 periods, the data were Fourier analyzed to allow comparison with LST and PSE results.

4.1. Linear test case

For the linear test case the amplitude was set to $A = 1 \times 10^{-4}$ and the phase to $\theta = 0$. In Fig. (4) the amplitude distribution in the normal direction of the streamwise and normal velocity components are plotted at the streamwise position $x = 3.9905$. The results obtained by DNS and LST are nearly the same. The maximum amplitude, phase change and exponential decay are all in very good agreement with LST. The quality of the results can also be observed in Fig. (5) where the phase relationships with respect to y at the same x position are plotted. Both the phase distribution for the streamwise and normal velocity components are shown.

Figure (6) shows the streamwise distribution of the growth rate obtained with the DNS code and with a LST analysis. The small deviation observed is attributed to non parallel effects that are not taken into account when the Orr-Sommerfeld equation is solved. The growth rate distribution obtained with a PSE code, that can also take into account nonparallel effects of boundary layer growth, is also shown. The same deviation from LST is observed in the PSE results.

4.2. Non Linear Test Case

In order to simulate the propagation of nonlinear Tollmien-Schlichting waves, a finite amplitude disturbance was introduced in the flow field. The propagation of finite amplitude TS waves may be described by a weakly nonlinear theory such as a nonlinear PSE analysis. The propagation of TS waves is characterized by the evolution of a fundamental wave accompanied by the growth of higher harmonics. In the following analysis, DNS results for amplification of a fundamental and higher harmonics, as well as for the variation of the growth rate and eigenfunctions for different harmonics are compared to PSE results.

In Fig. (7) the variation of the streamwise velocity amplitude in the streamwise directing for the fundamental and 3 harmonics are plotted. The initial amplitude of the disturbance was set to $A = 1 \times 10^{-3}$. A good agreement between DNS and PSE results can be observed after the streamwise position $x = 3.0$. The deviation that is observed before this position is explained by the existence of a transient region where the disturbances introduced

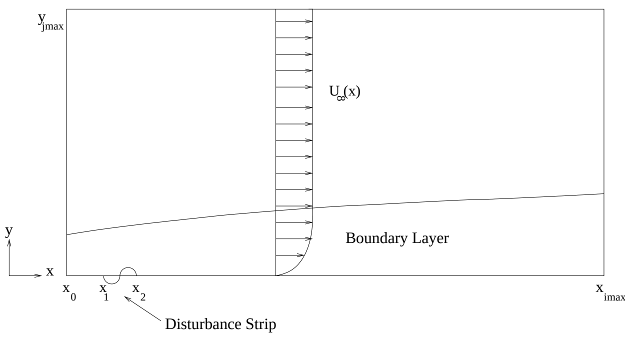

Figure 3: Integration domain for the flat plate boundary layer.

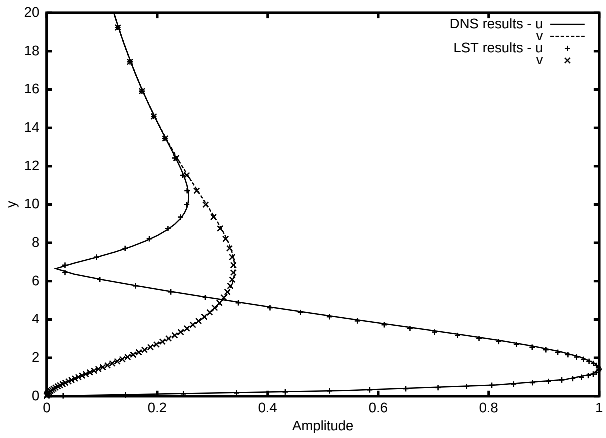

Figure 4: Comparison between DNS and LST results disturbances eigenfunctions in the streamwise and normal directions.

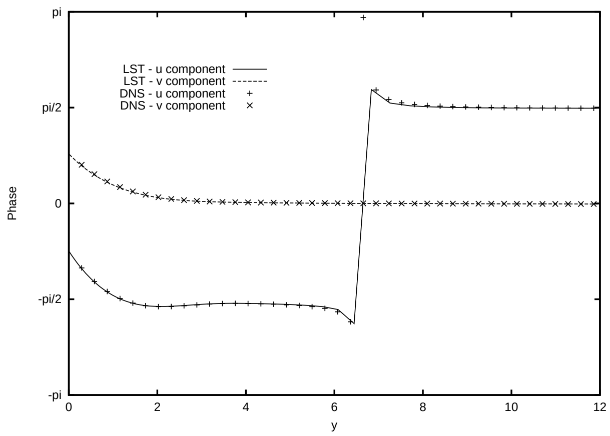

Figure 5: Comparison between DNS and LST results for the phase distribution.

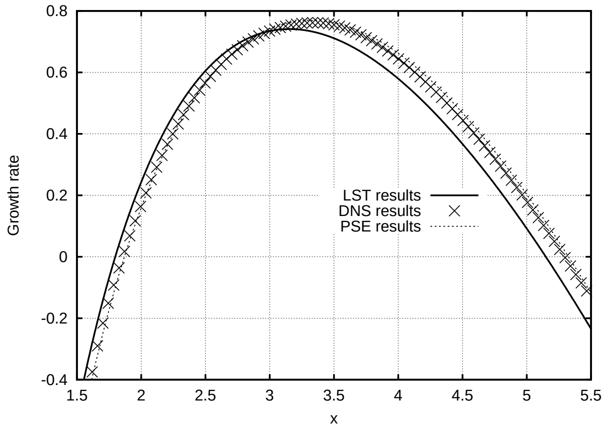

Figure 6: Comparison between DNS, PSE and LST results for the growth rate.

numerically in the flow field adjust to the nonlinear set of equations. In the PSE analysis a single fundamental mode is specified as initial condition for the marching solution. Since the initial amplitude correspond already to a nonlinear problem, the disturbance field has to adjust in a finite transient region where higher harmonics are generated. In the DNS analysis the disturbances are introduced in a suction and blowing strip and this signal has to be filtered by the governing equations such that, after the transient region the fastest growing TS wave is the only wave remaining.

During the initial transient region the first harmonic is also an unstable mode and has its own growth rate according to LST. In this region the growth of this mode is governed by both the nonlinear forcing and its linear exponential growth. As a result the amplification does not correspond to a purely nonlinear growth or to a purely linear growth of a single TS wave with twice the frequency of the imposed fundamental.

The comparison between the growth rate variation in streamwise direction for three different initial amplitudes are shown in Fig. (8). The Three different values of amplitude tested were $A = 1 \times 10^{-3}$, $A = 5 \times 10^{-4}$, $A = 1 \times 10^{-4}$. The last test case correspond closely to a linear problem. It can be observed that as the disturbance amplitude increases, the streamwise position corresponding to the second branch of the neutral curve moves forward as a consequence of the nonlinear effects.

Figures. (9) to (12) present the streamwise and normal velocity profiles for the amplitude $A = 1 \times 10^{-3}$ at the streamwise position $x = 3.9905$. Figure (9) corresponds to the amplitude of the fundamental mode and Figs. (10) to (12) correspond to the first, second and third harmonics respectively. The results show a very good agreement between DNS and PSE results. The distance from the wall where the maximum amplitude is observed, the position of phase change, as well as the maximum amplitude itself are all captured with very good accuracy. The amplitude of all modes have been normalized by the maximum amplitude of the fundamental streamwise component.

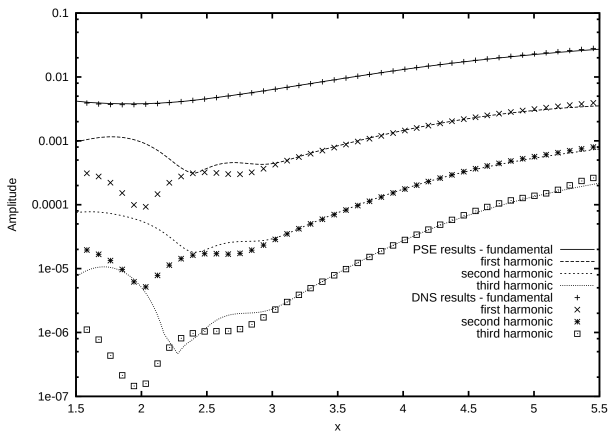

Figure 7: Comparison between nonlinear DNS and PSE results. Streamwise velocity component amplitude variation in the streamwise direction.

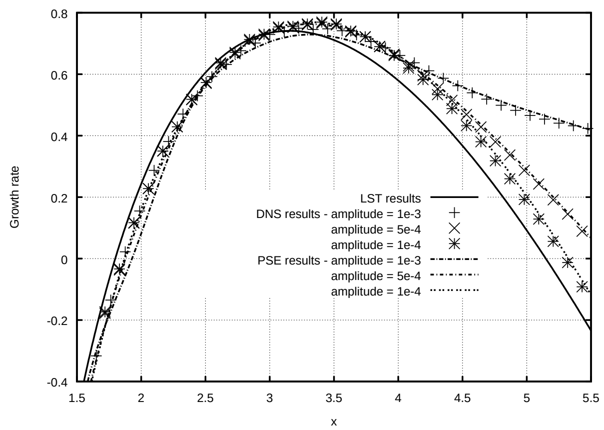

Figure 8: Comparison between nonlinear DNS and PSE results. Growth rate variation in the streamwise direction.

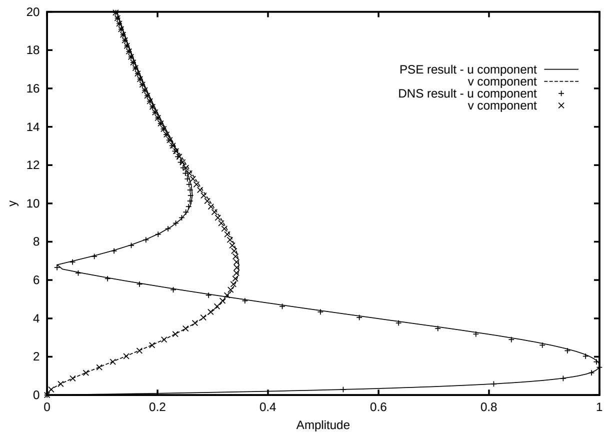

Figure 9: Comparison between nonlinear DNS and PSE results. Amplitude distribution of streamwise and wall normal velocity components for mode (1,0) at x=3.9905.

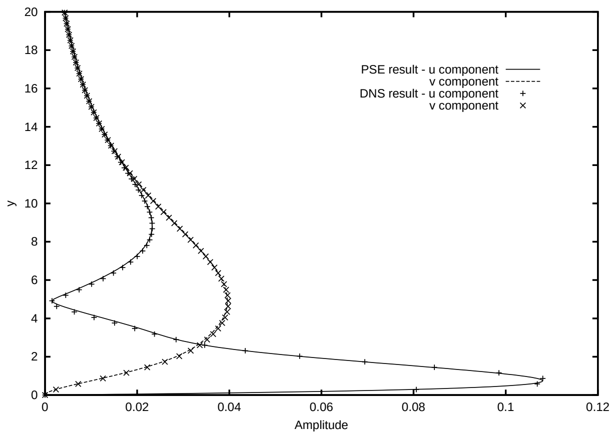

Figure 10: Comparison between nonlinear DNS and PSE results. Amplitude distribution of streamwise and wall normal velocity components for mode (2,0) at x=3.9905.

5. Conclusions

In the present paper a numerical method for solving a two-dimensional incompressible flow that is applicable to investigation of laminar turbulent transition phenomena in a spatially growing boundary layer was presented. The code was verified against linear stability theory results for the propagation of small amplitude Tollmien-Schlichting waves. Nonlinear results obtained with the code were compared to PSE results. The nonlinear evolution of the fundamental mode and higher harmonics were investigated and very good agreement with nonlinear PSE results were obtained.

The next step in the development of a three-dimensional code is to introduce a spectral approximation in the spanwise direction that will allow the simulation of oblique waves propagation. The resulting code will be used to study transition to turbulence in boundary layer and shear layer flows.

6. Acknowledgments

The first author would like to acknowledge all the transition research group of the Institut fur Aerodynamic and Gasdynamic (IAG) from Universitat Stuttgart. The first and the second authors would like to acknowledge the financial support received from FAPESP.

7. References

Bestek, H., 1980, “Numerische Untersuchungen zur nichtliearen räumlichen Störungsanfachung in der ebenen Poiseuille-Strömung”, PhD thesis, University of Stuttgart.

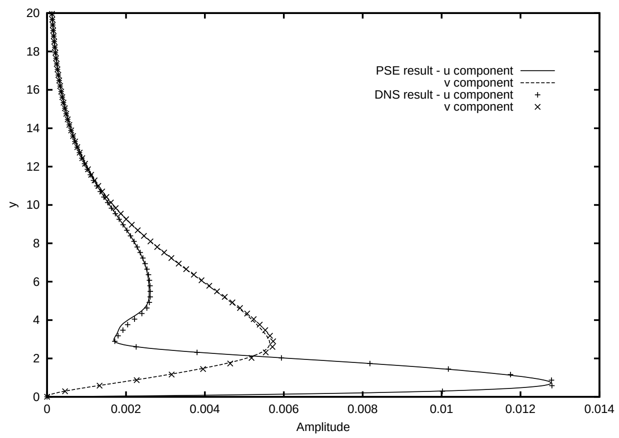

Figure 11: Comparison between nonlinear DNS and PSE results. Amplitude distribution of streamwise and wall normal velocity components for mode (3,0) at x=3.9905.

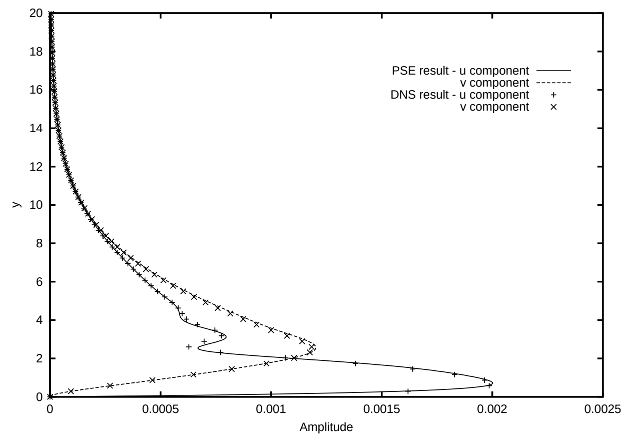

Figure 12: Comparison between nonlinear DNS and PSE results. Amplitude distribution of streamwise and wall normal velocity components for mode (4,0) at x=3.9905.

Biringen, S. and Laurien, E., 1991, Nonlinear Structures of Transition in Wall-Bounded Flows, “Appl. Num. Mathematics”, Vol. **7**, pp. 129–150.

Davies, C., Carpenter, P., and Lockerby, D., 1999, A novel velocity-vorticity method for simulating boundary-layer disturbance evolution and control, “The IUTAM 99 Symp. on Laminar-Turbulent Transition”, Arizona, USA.

Farouk, B. and Fusegi, T., 1985, A Coupled Solution of the Vorticity–Velocity Formulation of the Incompressible Navier–Stokes Equations, “Int. J. for Numerical Methods in Fluids”, Vol. **5**, pp. 1017–1034.

Fasel, H. F., Rist, U., and Konzelmann, U., 1990, Numerical Investigation of the Three-Dimensional Development in Boundary-Layer Transition, “AIAA Journal”, Vol. 28, No. 1, pp. 29–37.

Fezer, A. and Kloker, M., 1999, Spatial Direct Numerical Simulation of Transition Phenomena in Hypersonic Flat-Plate Boundary Layers at Flight Conditions, “The IUTAM 99 Symp. on Laminar-Turbulent Transition”, Arisona, USA.

Gmelin, C., Rist, U., and Wagner, S., 1999, DNS of Active Control of Disturbance in a Boundary-layer, “The IUTAM 99 Symp. on Laminar-Turbulent Transition”, Arisona, USA.

Guschin, V., Kostomarov, A., Matyushin, P., and Pavlyukova, E., 1999, Direct Numerical Simulation of 2-D/3-D Transition in the Separated Fluid Flows Around a Sphere, “The IUTAM 99 Symp. on Laminar-Turbulent Transition”, Arisona, USA.

Hu, S. H. and Zhong, X., 1999, Nonparallel Stability Analysis of Hypersonic Flow over a Swept Blunt Leading Edge, “37th AIAA Aerospace Sciences Meeting and Exhibit”, Reno, NV.

Kloker, M., Konzelmann, U., and Fasel, H., 1993, Outflow Boundary Conditions for Spatial Navier-Stokes Simulation of Transition Boundary Layer, “AIAA Journal”, Vol. 31, No. 4, pp. 620–628.

Kopal, Z., 1961, “Numerical Analisys”, 2nd edition, Chapman & Hall.

Laurien, E. and Kleiser, L., 1989, Numerical Simulation of Boundary-Layer Transition and Transition Control, “J. Fluid Mechanics”, Vol. **199**, pp. 403–440.

Lele, S., 1992, Compact Finite Difference Schemes with Spectral-like Resolution, “J. Computational Physics”, Vol. **103**, pp. 16–42.

Mahesh, K., 1998, A Family of High Order Finite Difference Schemes with Good Spectral Resolution, “J. Computational Physics”, Vol. **145**, pp. 332–358.

Medeiros, M. A. F. and Gaster, M., 1999, The production of sub-harmonic waves in the nonlinear evolution of wavepackets in boundary layers, “J. Fluid Mech.”, Vol. 397, pp. 301–318.

Meitz, H. L. and Fasel, H. F., 2000, A compact-difference scheme for the Navier-Stokes equations in vorticity-velocity formulation., “J. Comp. Phys.”, Vol. **157**, pp. 371–403.

Mendonça, M. T., 2000, “Laminar Flow Stability: Linear Theory”, chapter 5, pp. 98–147, II Brazilian School of Transition and Turbulence. ABCM.

Mendonça, M. T., 2000, Parabolized Stability Equation: A Review, “National Congress of Mechanical Engineering - CONEM 2000”, Natal - RN, Brazil.

Messing, R., Kloker, M., and Wagner, S., 1999, Effect of Suction Through Arrays of Holes on a 3-D Boundary Layer Investigated by Spatial Direct Numerical simulation, “The IUTAM 99 Symp. on Laminar-Turbulent Transition”, Arisona, USA.

Meyer, D., Rist, U., Gaponenko, V., Kachanov, Y., Lian, Q., and Lee, C., 1999, Late-Stage Transition

Boundary-Layer Structures. Direct Numerical Simulation and Experiment, "The IUTAM 99 Symp. on Laminar-Turbulent Transition", Arisona, USA.

Souza, L. F., Mendonça, M. T., and Medeiros, M. A. F., 2001, A high resolution Navier Stokes solver for hydrodynamic stability analysis, "22nd CILAMCE, Iberian Latin-American Congress on Computational Methods in Engineering", Campinas - SP.

Spalart, P. R., 1989, Direct Numerical Study of Crossflow Instability, "The IUTAM 90 Symp. on Laminar-Turbulent Transition", Toulouse, France.

Stemmer, C. and Kloker, M., 1999, Later Stages of Transition of an Airfoil Boundary-Layer Excited by a Harmonic Point Source, "The IUTAM 99 Symp. on Laminar-Turbulent Transition", Arisona, USA.

Wassermann, P. and Kloker, M., 1998, Direct Numerical simulation of the Development and Control of Boundary-Layer Crossflow Vortices, Nilsche, W. and Hilbig, R., editors, "New Results in Numerical and Experimental Fluid Dynamics", Berlin.

Wassermann, P. and Kloker, M., 1999, DNS Investigation of the Development and Control of Crossflow Vortices in a 3-D Boundary-Layer, "The IUTAM 99 Symp. on Laminar-Turbulent Transition", Arisona, USA.

Whang, C. and Zhong, X., 1999, Direct Numerical Simulation of Görtler Instability in Hypersonic Boundary-Layers, "The IUTAM 99 Symp. on Laminar-Turbulent Transition", Arisona, USA.

Zang, T. A., Krist, S. E., and Hussaini, M. Y., 1989, Resolution Requirements for Numerical Simulations of Transition, "J. of Scientific Computing", Vol. **4**, pp. 197–217.

Zhang, H. and Fasel, H., 1999, Spatial Direct Numerical Simulation of Görtler Vortices, "AIAA Fluid Dynamics Conference", Norfolk, USA.

Zhong, X., 1999, DNS of Boundary-Layer Receptivity to Freestream Sound for Hypersonic Flows Over Blunt elliptical Cones, "The IUTAM 99 Symp. on Laminar-Turbulent Transition", Arisona, USA.